



# Comparative Measurements of Physical and Mechanical Properties of AA6082 Based Composites Reinforced with B<sub>4</sub>C and SiC Particulates Produced via Stir Casting

Gurpreet Singh<sup>1,3</sup> · Neeraj Sharma<sup>2</sup> · Sanjeev Goyal<sup>3</sup> · Rakesh Chandmal Sharma<sup>2</sup>

Received: 8 January 2020 / Accepted: 23 February 2020 / Published online: 11 March 2020  
© The Korean Institute of Metals and Materials 2020

## Abstract

AA6082/B<sub>4</sub>C and AA6082/SiC were prepared via stir casting accompanied by an inert-gas to prevent oxidation. The samples for both the composites were produced with varying wt% of 0, 5, 10, 15 and 20 of B<sub>4</sub>C and SiC for their respective composites. This work gives emphasis on the comparative measurements of hardness, tensile strength, percentage elongation, Impact strength, density and porosity of the AA6082/B<sub>4</sub>C and AA6082/SiC composites. The microstructure was studied using X-ray diffractometer and SEM. The micro hardness in AA6082/B<sub>4</sub>C composites increases to 15.8% and the increase in AA6082/SiC composites is 11.9% only when compared with the base alloy whereas the increase in ultimate tensile strength for B<sub>4</sub>C and SiC reinforced composites was reported to be 31% and 19.1% respectively. At 20 wt% of B<sub>4</sub>C, hardness and tensile strength of AA6082/B<sub>4</sub>C composite tends to decrease due to the development of clusters and increased porosity. The transformation in the nature of material from ductile to brittle decreases the impact strength and the resistance in the flow ability presented by the hard ceramic particles lowers down the percentage elongation. Density reduces from 2.67 g/cm<sup>3</sup> in base alloy to 2.48 g/cm<sup>3</sup> in AA6082/B<sub>4</sub>C and 2.56 g/cm<sup>3</sup> in AA6082/SiC composites respectively. The formation of voids in AA6082/SiC composites makes it less porous than AA6082/B<sub>4</sub>C composites and this was because of the more agglomeration in SiC composites due to their high density.

**Keywords** AA6082/B<sub>4</sub>C · AA6082/SiC · Microstructure · Hardness · Tensile strength · Percentage elongation · Impact strength · Density · Porosity

## 1 Introduction

Aluminium matrix composites (AMC's) have been used extensively in various sectors like automobile, marine, defense, aerospace, structures and transport where the high strength of material is required to bear the induced stresses [1–3]. The widespread use of AMC's is attributed to its excellent mechanical properties [4, 5]. It was also observed in the past

research that the natural ductility of aluminium alloy tends to diminish with the gradual addition of reinforcements like SiC, Al<sub>2</sub>O<sub>3</sub>, TiB<sub>2</sub> or graphite [6]. SiC as reinforcement have drawn much attention of the researchers over the years because it is regarded as one of the finest to form chemical bonding with aluminium matrix and also has admirable physical properties [7] while B<sub>4</sub>C exhibits properties like low density, high stiffness and hardness [8]. Various researchers in the past used different aluminium alloys to fabricate composites reinforced with ceramic particles to evaluate their physical and mechanical properties. Ravikumar et al. [9] worked on the mechanical characterization of Al/TiC composites to study the mechanical composites and the results show that the density, impact strength and elongation falls with the TiC addition in the composites. In another research conducted by Krishna et al. [10], AMC's were fabricated using varying wt% of 6, 8, 10, 12 of B<sub>4</sub>C particulates to study the composite characterization and it was found that the tensile strength and harness gradually increases by adding the particles in the matrix. Ghanbari et al.

✉ Gurpreet Singh  
gurpreet.er85@gmail.com

<sup>1</sup> Department of Automobile Engineering, Amity University  
Uttar Pradesh, Noida, U.P. 201313, India

<sup>2</sup> Department of Mechanical Engineering, Maharishi  
Markandeshwar (Deemed to be University),  
Mullana, Ambala, Haryana 133207, India

<sup>3</sup> Department of Mechanical Engineering, YMCA University  
of Science and Technology, Faridabad, Haryana 121006,  
India

[11] studied the composites produced with aluminum and SiC particulates and it was reported that the hardness increases due to the effect of heat treatment along with the formation of fine grains in the structure of the composites. In a study conducted by Aigbodion and Hasan [12], the effect of SiC particulates have been studied and the authors found that tensile strength, hardness and porosity in composites increases to a significant level but at the same time the density and impact strength decreases in the composites. Rahman and Rashid [13] fabricated aluminium composites using varying wt% of SiC (0, 5, 10 and 20 wt%) and observed that the hardness and tensile strength was maximum at 20 wt% of SiC. Rahman and Rashid [13] also found that the tensile strength was higher in case of 5% SiC as compared to the composite having 10 wt% of SiC. Kumar et al. [14] worked on the machining and mechanical behavior of hybrid composites produced using MoS<sub>2</sub> and B<sub>4</sub>C particles and the experiments were carried out to study the surface roughness and the forces developed in the turning operation of composites. The results obtained from the study of Kumar et al. [14] shows that the addition of ceramic particles increases the surface roughness and cutting forces in the material. Tan et al. [15] employed different particle size of SiC for the development and experimentation of Al/SiC composites and exposed that increasing the particle size of SiC from 7 to 250 µm decreases the bending strength of the composites. Afkham et al. [16] performed the detailed investigation on aluminium matrix composites using alumina nanoparticles as reinforcement and reported an increase in the tensile strength and hardness in the fabricated composites. Senel et al. [17] used graphene nanoplatelets (GNPs) and silicon carbide (SiC) as reinforcements to fabricate Aluminium composites and the hardness and the compressive strength was investigated. Senel et al. [17] Reported that both the hardness and the compressive strength of the composites increases with the increase of SiC (0–30 wt%) and GNPs (0.1–0.5 wt%) in the metal matrix. Singh and Goyal [18] worked on the hybrid composites produced using the base alloy AA6082 and the particulates of SiC and B<sub>4</sub>C to investigate the mechanical behavior and mechanical properties of the composites and it was reported that the gradual addition of particles helps in enhancing the hardness of the composites along with the reduction in the rate of removal of material.

In the present research AA6082 was used as the base alloy as it is regarded as one of the strongest alloy due to the presence of silicon in it [18]. AA6082 finds application in many structural parts where high strength is essential such as bridges, cranes, trusses and transport applications [19]. As reported earlier, few works are available on SiC

and B<sub>4</sub>C reinforced composites where researchers worked on different aluminium alloys but no publication till date has drawn a parallel comparison in terms of mechanical and physical properties of composites developed from same alloy and different reinforcements. In view of this, the authors would like to give more emphasis on the mechanical behavior and characterization of aluminium composites and makes an attempt to expand the knowledge in this area by drawing a parallel comparison on the physical and mechanical properties of the AA6082/SiC and AA6082/B<sub>4</sub>C composites that include the study of density, porosity, micro hardness, tensile strength, percentage elongation and impact strength. In the presents work, the authors have made an attempt to fabricate AA6082/B<sub>4</sub>C and AA6082/SiC composites separately through conventional stir casting using varying wt% of 0, 5, 10, 15 and 20 for both SiC and B<sub>4</sub>C particulates. Further, the microstructure of the composites was studied using SEM micrographs and XRD patterns. This work intends to assess how the properties of the two composites differ on using the same base alloy under similar testing conditions.

## 2 Materials and Methods

### 2.1 Starting Material

AA6082 was taken as the base alloy whose details are given in Tables 1 and 2. The fine particulates of B<sub>4</sub>C and SiC having mesh size of 35 microns were added in the matrix to produce the composites.

The properties of both the particulates are shown in Table 3 and their SEM images are shown in Fig. 1. AA6082/B<sub>4</sub>C and AA6082/SiC composites were produced using conventional stir casting accompanied by an inert gas to prevent oxidation. The samples were produced with varying wt% of 0, 5, 10, 15 and 20 of both B<sub>4</sub>C and SiC for their respective composites.

**Table 2** Mechanical properties of AA6082

Tensile strength (MPa)	Proof stress (0.2% MPa)	Density (g/cm <sup>3</sup> )	Vickers hardness (HV)	% Elongation (min%)
320	310	2.67	100	9

**Table 1** Chemical composition of AA6082 in wt%

Element	Mg	Si	Mn	Fe	Cu	Cr	Zn	Ti	Vn	Al
Content (wt%)	0.69	0.91	0.56	0.23	0.06	0.035	0.098	0.019	0.01	97.4

**Table 3** Details of SiC and B<sub>4</sub>C particulate

Reinforce-ment	Average particle size (μm)	Density (g/cm <sup>3</sup> )	Melting point (°C)	Hardness (HV)
SiC	35	3.20	2700	285
B <sub>4</sub> C	35	2.52	2450	305

## 2.2 Fabrication of Composites

The schematic diagram of the conventional stir casting apparatus for the fabrication of composite is shown in Fig. 2. For the fabrication of aluminium composite, small rectangular pieces of aluminium base material were cut and weighted on digital weight machine. After accurate measurement of 1000 g of Al for each specimen of composite, the alloy was heated in the furnace. The furnace was heated up to a temperature of 850 °C, so that aluminium in the crucible melted completely. The reinforcement particles used in the present work was pre-heated for 3–4 h up to 200–250 °C so

as to evaporate the moisture content. Argon gas was used while adding the particles in the molten metal as a measure to prevent oxidation. As magnesium is assumed as a good wettability agent, so 2 wt% Mg was also blended with the aluminium alloy [20].

The mixture containing the molten alloy, particulates and the magnesium was stirred unceasingly with the assistance of a graphite stirrer for 8–10 min. The stirring speed was kept at 450 rpm. After complete mixing of particulates with the molten metal, the homogeneous mixture (aluminium alloy with reinforcement) was transferred in a pre-heated sand mold where it solidifies in open atmosphere. After solidification of mixture, the composite was taken out of the mold and machined to carry out the experimental work. All the samples were prepared using the same methodology.

## 2.3 Microstructure Samples

Samples having circular cross-section were machined through wire EDM to carry out the microstructural study. Abrasive paper of different grades viz.: 400, 600 and 1000

**Fig. 1** **a** SEM micrographs of SiC particles and **b** SEM micrographs of B<sub>4</sub>C particles

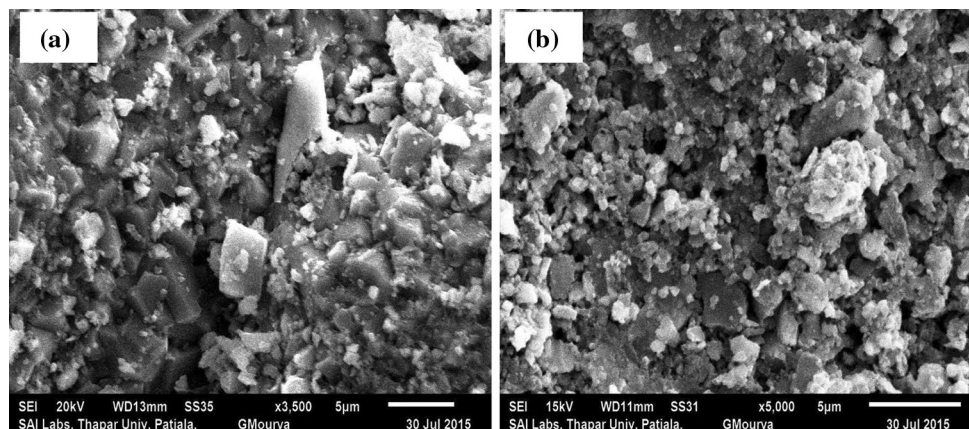
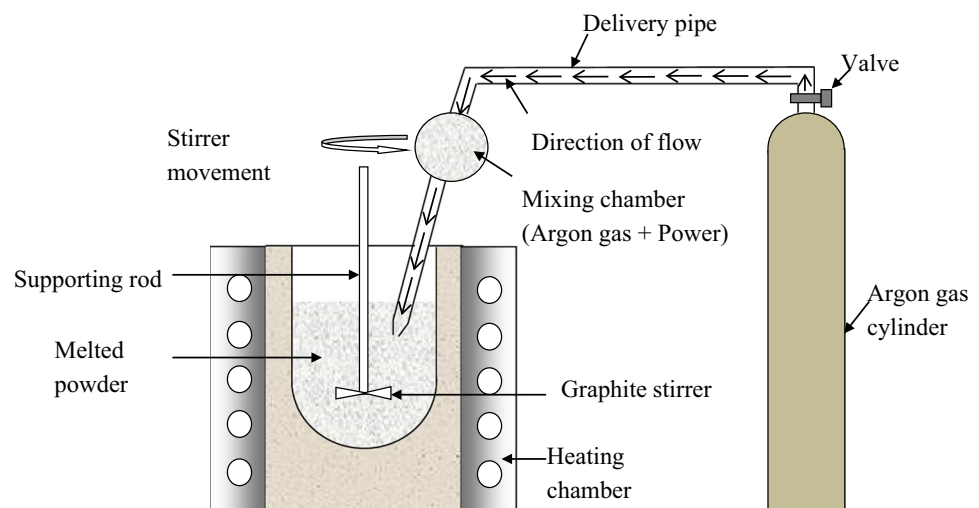


**Fig. 2** Schematic of stir casting apparatus



were used for the grinding of samples. To reveal the micrograin, the samples must be etched properly. In present work, Keller's solution having 3 ml HCl, 2 ml HF, 175 ml H<sub>2</sub>O and 20 ml HNO<sub>3</sub> was used. Single crystal monochromator at an angle of 20° to 110 °C was used for XRD analysis. Jeol make JSM-6510LV scanning electron microscope was employed to capture the micrographs.

## 2.4 Hardness Test Samples

Vickers hardness tester which is a Mitutoyo (Japan) make was used to examine the hardness of the composites. The test method ASTM E-384 was employed for this purpose. In this, a diamond indenter was used to spot the impression which was measured to get the hardness. The specimen for Vickers hardness testing was machined with square cross-section.

Each specimen undergoes the hardness tests for 3 times and the average value has been taken. The harness is evaluated through Eq. 1.

$$HV = \frac{1.854F}{d^2} \quad (1)$$

where F, force applied; d, indentation depth.

## 2.5 Tensile Specimen and Elongation

The specimen used for the tensile test was made as per ASTM-E8 standard [21] and the experiments were conducted on universal testing machine. The schematic diagram of tensile specimen is shown in Fig. 3 where L<sub>0</sub> = 60 mm, thickness = 6 mm, L<sub>C</sub> = 80 mm, b = 10 mm, and R = 10 mm. The elongation was determined with the help of an axial extensometer. Its measuring accuracy exceeds all requirement set down by standard EN ISO 9513. The measuring range for the extensometer was up to 3 mm and was suitable for Flat Specimens. The percentage elongation was measured from Eq. 2 using the initial gage length and the final gage length of each specimen that undergoes the tensile tests.

Percentage elongation

$$= \frac{\text{final gage length} - \text{initial gage length}}{\text{initial gage length}} \times 100 \quad (2)$$

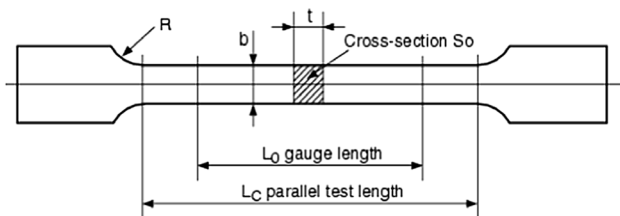


Fig. 3 Schematic of flat tensile test specimen

## 2.6 Impact test Samples

ASTM E23 standard was used for sample preparation. The testing machine having ASI make is of pendulum type with a capacity of 185 joules. The impact tester provides a range of energy varying from 0 to 300 J. The schematic diagram of impact specimen (56 mm × 10 mm × 10 mm) is shown in Fig. 4. The depth of notch is taken as 2 mm and the tip radius of 0.25 mm at an angle of 45°. Multi-readings were carried out and the average of three has been taken.

## 2.7 Density

The density was determined using the mass and the volume of a specimen as given in Eq. 3

$$\text{Density (g/cm}^3\text{)} = \frac{\text{Mass}}{\text{Volume}}. \quad (3)$$

Initially a vessel was filled with a known quantity of water up to a certain level. A hole was provided in the vessel just above the water level and the specimen was dipped into the vessel. As the specimen dropped into the vessel, some of the water comes out of the vessel through the hole. The volume of the water that comes out of the vessel is equal to the volume of the specimen. The graduated test tube was used to measure the volume of water that comes out from vessel. Mass of the sample was evaluated by weighing the sample and using the simple relation between mass and weight i.e. 1000 g equals to 9.81 Newton.

## 2.8 Porosity

The porosity is the void in between the particles. In this work, the apparent porosity of AA6082/B<sub>4</sub>C and AA6082/SiC composites was calculated experimentally. The steps involved in the experimental procedure are as follows:

1. *Determination of dry weight (D)* The test specimen was heated in the oven of 3 h at about 110 °C and

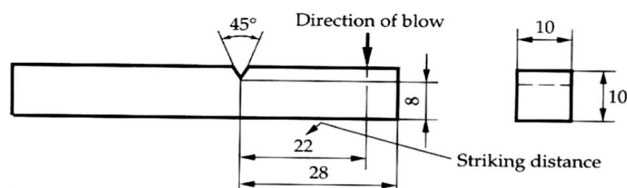


Fig. 4 Schematic of samples for impact testing

then weighted to an accuracy of 0.01 g to get the dry weight D.

2. *Saturation* Place the test specimen in a container filled with water and boils it for 2 h. During the boiling of water, the specimen should be dipped in water completely and also not in contact with the bottom of the container. After boiling, the specimen was kept suspended in water for another 4–5 h so as to lower down its temperature.
3. *Suspended weight (S)* After saturation, weight the test specimen while suspended in water to an accuracy of 0.01 g. This weighing was achieved by suspending the specimen in a loop of copper wire hung from one arm of the digital balance hinged on the stand.
4. *Saturated weight (W)* Immediately after obtaining the suspended weight S, remove the specimen from the water and blot lightly with a moistened clean towel to remove all the water droplets from the surface of the test specimen. After this, the specimen was weighted in air to obtain the saturated weight W. The blotting process should be performed very lightly otherwise excessive blotting will induce error by withdrawing water from the pores of the specimen.

To measure the apparent porosity of the composites, Eq. 4 given below was employed [12]

$$\text{Porosity } (P) = \frac{W - D}{W - S} \times 100 \quad (4)$$

### 3 Results and Discussion

#### 3.1 X-Ray Analysis and Microstructural study

XRD of AA6082/B<sub>4</sub>C was depicted in Fig. 5a–d with the variation of percentage reinforcement. The XRD patterns show the presence of Al<sub>3</sub>BC and B<sub>4</sub>C accompanied by Al and Si. The peaks of Al<sub>3</sub>BC are smaller as compared to B<sub>4</sub>C, Al and Si as it is a by-product which forms due to the reaction between Al and B<sub>4</sub>C particles. Figure 6a–d shows the patterns for AA6082/SiC composites where the peaks of Al, Al<sub>4</sub>C<sub>3</sub>, Si and SiC were observed. The XRD patterns show an increase in the peaks of SiC with the gradual increase of particles in the matrix. The production of the Al<sub>4</sub>C<sub>3</sub> phase adversely affects the fabrication of composite due to aluminium hydroxide (in the presence of moisture). This aluminium hydroxide degrades the quality of the composites. The formation of Al<sub>4</sub>C<sub>3</sub> can be minimized after optimizing the process parameters [22], coating the reinforcement particles with SiO<sub>2</sub>, or improvement in composition of the aluminium matrix [23].

SEM micrographs of the composites with varying wt% of 0, 5, 10, 15 and 20 are shown in Figs. 7a–d and 8a–d where it is evident that the mixture attained was significantly homogeneous. However, for higher percentage reinforcement, the clustering of the particles was observed. The clusters of SiC were found in the microstructure of AA6082/SiC composites at few places and the possible reason for this agglomeration was the higher density of SiC (3.20 g/cm<sup>3</sup>) as compared to aluminium (2.67 g/cm<sup>3</sup>). The agglomeration of particles in AA6082/B<sub>4</sub>C is comparatively less due to lower density of B<sub>4</sub>C particles which helps in better scattering of particles with the matrix. Microstructure of both the composites consists of very partial voids which show a good interfacial bonding among the metal and particles. The continuous stirring operation performed to obtain the homogeneous mixture also helped to eliminate the formation of oxide which is also evident from the micrographs. The particles get well settled with in the molten matrix during the solidification of the composites. No major casting defects such as shrinkage, large voids or pits were observed from the microstructural study.

#### 3.2 Micro-hardness

Micro-hardness of all the samples were measured using IS 1501-2002 standard. In this, the samples were initially cleaned and a load of 1 kg was applied for duration of 15 s. It is an important property of material by virtue of which material was characterized by strong intermolecular bonding.

Tables 4 and 5 show the micro-hardness results for AA6082/B<sub>4</sub>C and AA6082/SiC composites respectively. These results were the average of the three experiments conducted at different location of the specimen. Figure 9 shows the variation in hardness in composites with increase in reinforcement within the metal matrix. Plastic deformation of the material can be resisted by the accumulation of particles in the material [24]. The addition of both B<sub>4</sub>C and SiC improves the micro hardness of the composites. The hardness rises due to the high solidity of particles in the low solidity of matrix containing aluminium alloy and reinforced particles. Since B<sub>4</sub>C is a high performance monolithic ceramic particle with enormously high solidity and low specific weight, it provides better resistance to deformation as compared to SiC. The poor wettability of SiC as compared to B<sub>4</sub>C is another reason for the greater hardness of AA6082/B<sub>4</sub>C as compared to the SiC composites [25].

The hardness of the reinforcement particles i.e. SiC and B<sub>4</sub>C was equal to the 285 HV and 305 HV respectively, while at the same time base alloy gives the hardness value equal to the 101 HV. So, when the particulates were blended with the matrix then the hardness of the composites was increased. The results obtained from the research work depicted that the  $\mu$ -hardness of AA6082/B<sub>4</sub>C composite is

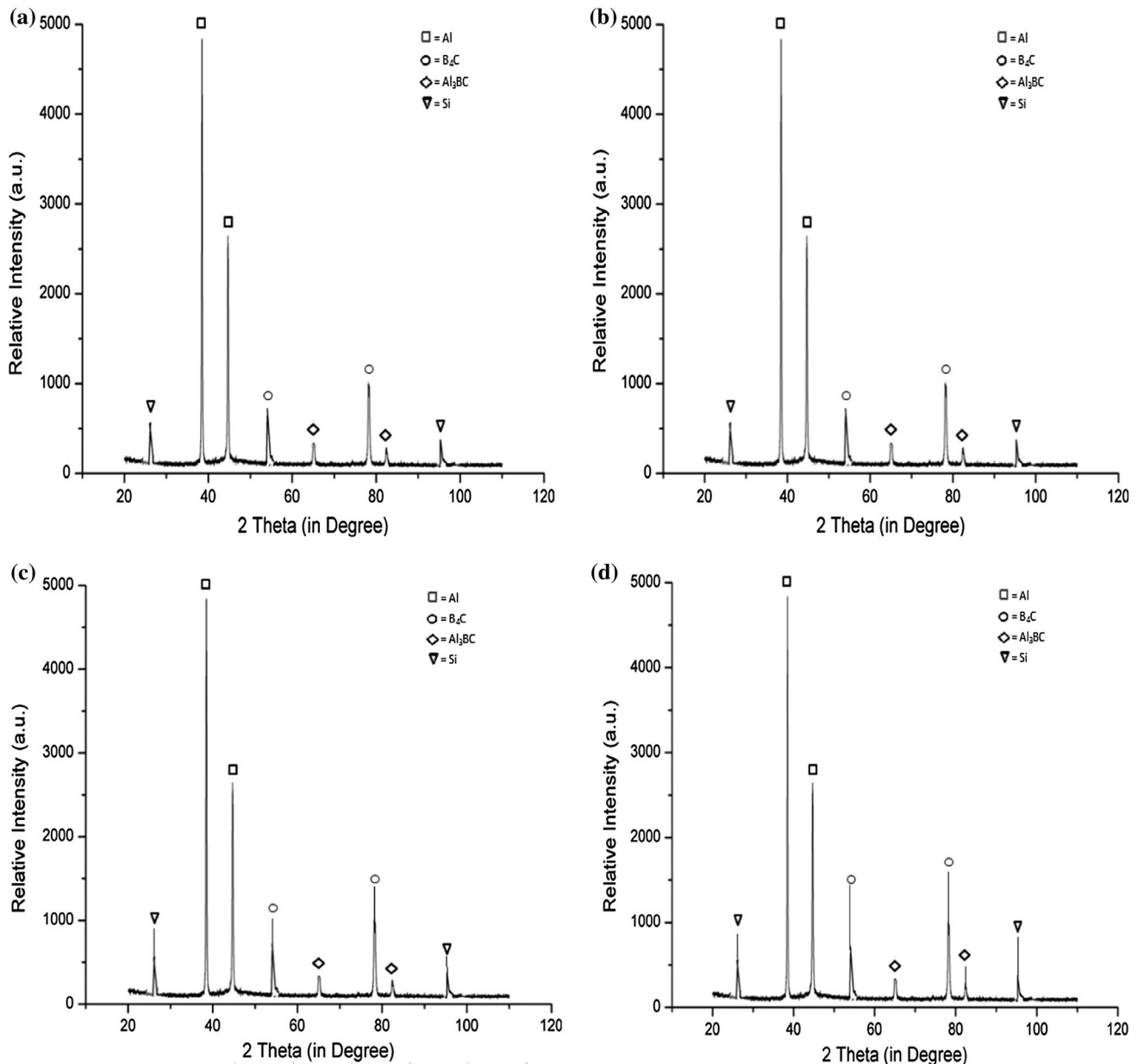


**Fig. 5** XRD patterns for **a** 5%, **b** 10%, **c** 15% and **d** 20% of AA6082/B<sub>4</sub>C composites

highest at 15 wt% of B<sub>4</sub>C which was equal to 117 HV and it goes down to 115 HV in composites having 20 wt% of B<sub>4</sub>C which could be due to the development of clusters within the composite at excessive addition of reinforced particles. AA6082/SiC composite gives maximum  $\mu$ -hardness at 20 wt% of SiC addition and it was 113 HV. The improvement in the hardness of composite helps to resist the plastic deformation in material. From the results obtained in the present work, it was found that the maximum improvement in the hardness is 15.8% (at 15 wt% of B<sub>4</sub>C) and 11.9% (at 20 wt% of SiC) for AA6082/B<sub>4</sub>C and AA6082/SiC composite respectively. The present work shows that after a particular

percentage of B<sub>4</sub>C addition in aluminium alloy, the hardness tends to decrease slightly due the clustering of B<sub>4</sub>C particles in aluminium matrix at some places. The brittle phase in B<sub>4</sub>C particulate was another criterion of the superior hardness of AA6082/B<sub>4</sub>C composite.

### 3.3 UTS and Percentage Elongation

Tensile test was performed according to ASTM-E8 standard on AA6082/B<sub>4</sub>C and AA6082/SiC composites on Texcare made computerized Tensile Testing Machine having a capacity of 500 kgf. Tables 6 and 7 depict the results for tensile

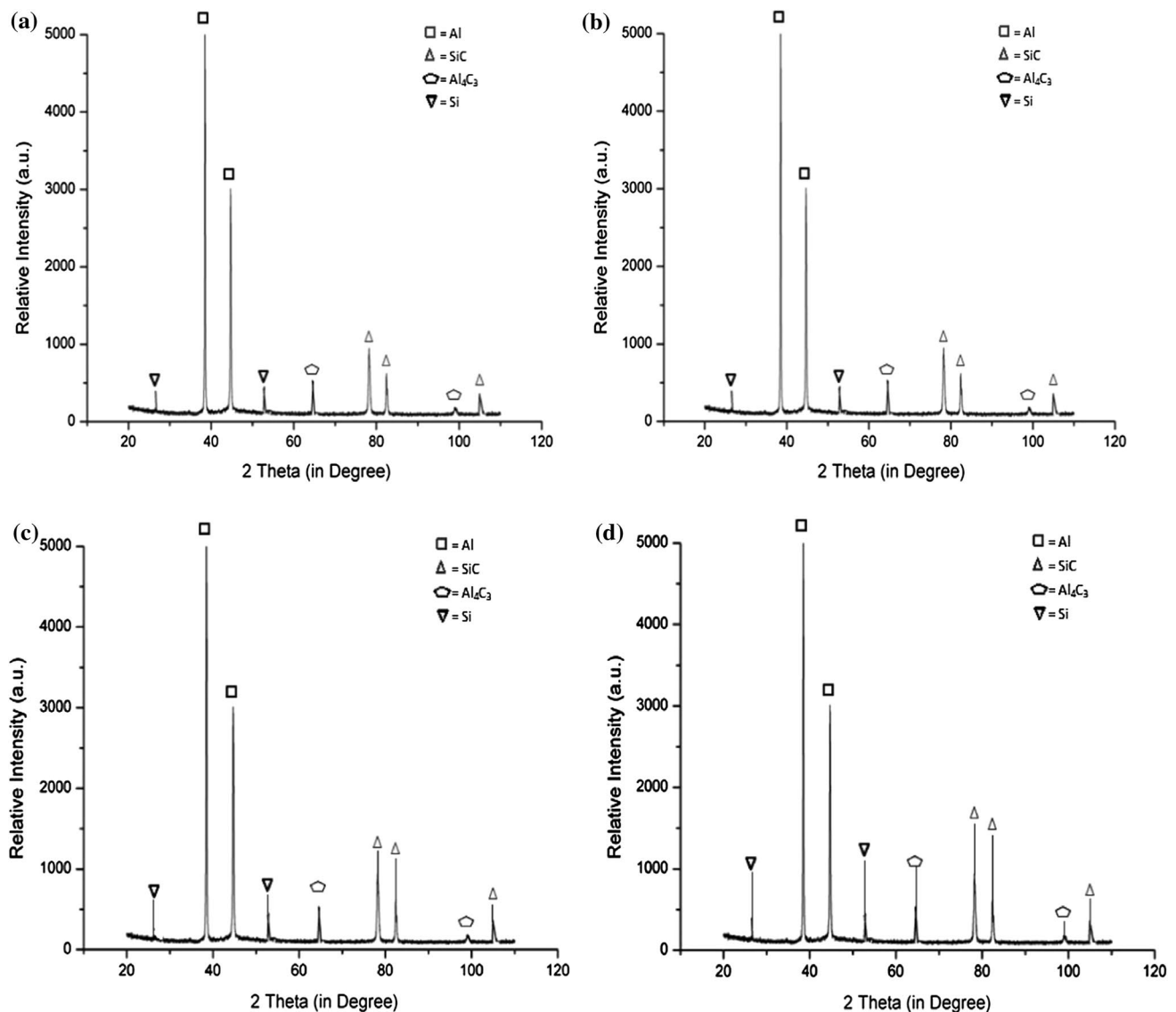


**Fig. 6** XRD patterns for **a** 5%, **b** 10%, **c** 15% and **d** 20% of AA6082/SiC composites

strength and % elongation of AA6082/ $B_4C$  and AA6082/SiC composites respectively.

The increase of ceramic particulates in the matrix increases the UTS of the composites and the reason behind this increment is the decent dispersion of the particles attained during the fabrication process. The UTS escalate to 417 MPa with 15% addition of  $B_4C$  particles form 318 MPa of base alloy, thereby increasing the UTS with 31%. The increase in  $B_4C$  (up to 20%) decreases the UTS due to the agglomeration of the reinforced particles [21]. Researchers in the past also reported increase in the tensile strength after addition of certain amount of reinforcement content. Mazahery and Shabani [26] also observed a rise in tensile strength up to 10% volume of  $B_4C$  but further addition of reinforcement results in

reduction of tensile strength. The cluster of particles in the matrix develops a weaker structure due to agglomeration of the particles. Also the porosity developed due to weaker structure reduces the UTS at 20%  $B_4C$ . Another reason for the increase of UTS in composites is the increase in stiffness value and capability to share more load on reinforced particles. As the proportion of reinforced particles increases in the composite, the stiffness of the composite also increases. This increment in the reinforcement particles also increases the capability of the composite to bear more loads due to sharing of the load on the reinforcement particles along with the base material. The SiC reinforced composite represent the increase in tensile strength but not as much momentous as of  $B_4C$ -reinforced composite. The 20% addition of SiC in aluminum matrix increases

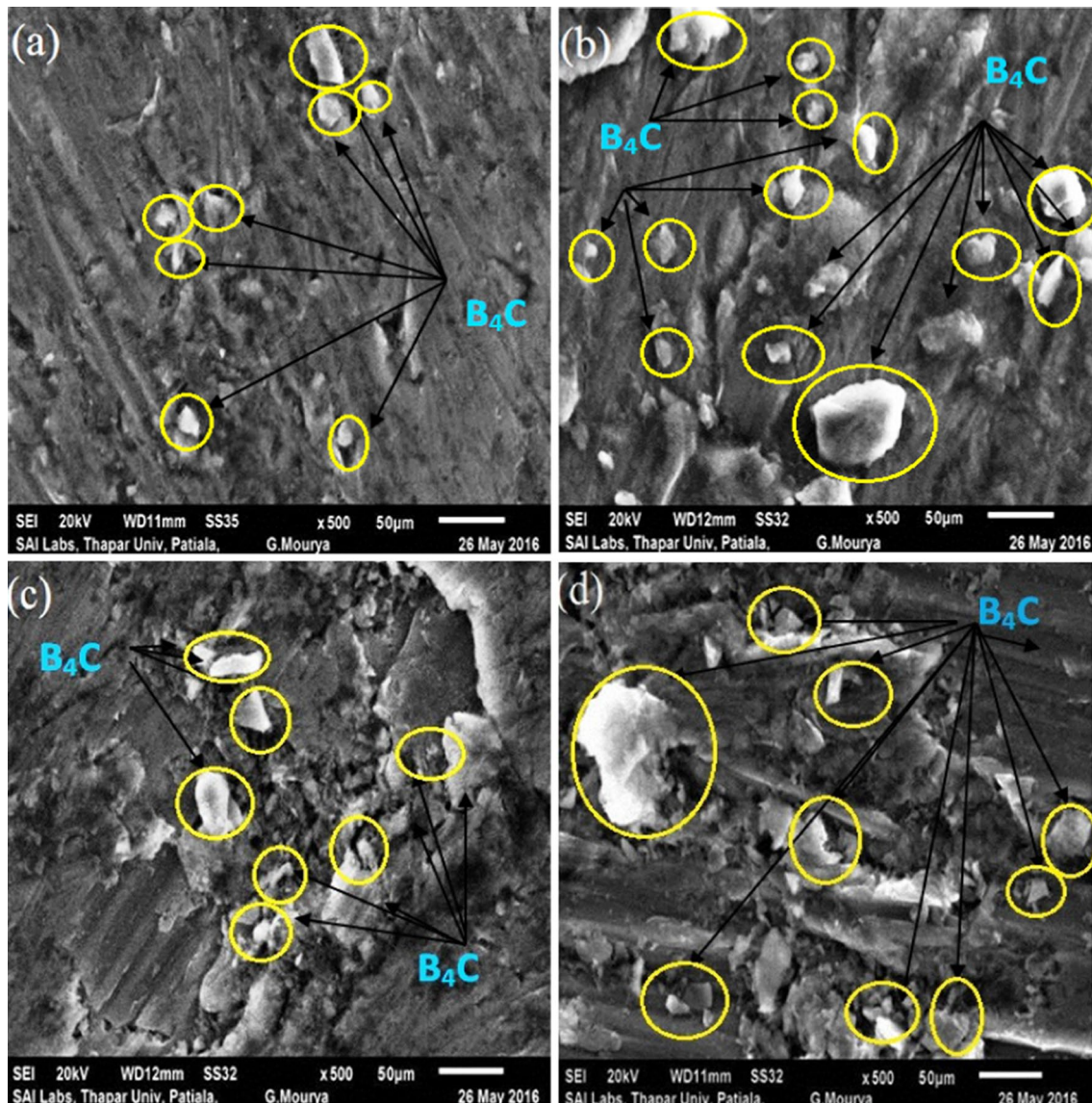


**Fig. 7** SEM micrographs for **a** 5%, **b** 10%, **c** 15% and **d** 20% of AA6082/B<sub>4</sub>C composites

the UTS by 19.1% and the value of tensile strength was recorded as 379 MPa. Figures 10 and 11 shows the variation of UTS and percentage elongation respectively.

Reduction in Percentage elongation was observed in the composites and this is because of the resistance in the flow ability presented by the hard ceramic particles. The reduction is more in B<sub>4</sub>C reinforced composites as compared to the composites reinforced with SiC. AA6082/B<sub>4</sub>C composite exhibit low percentage reinforcement as compared to AA6082/SiC due to the low density of B<sub>4</sub>C particles as compared to SiC particles. This reduction in percentage elongation is also attributed to the increase of UTS in the composites.

### 3.4 Impact Strength

The impact strength of the Al-composites was evaluated using Charpy test. Three identical samples were prepared for impact testing and the average of three has been selected for the analysis purpose. This strength is evaluated using the energy absorbed by the specimen during failure. Tables 8 and 9 gives the impact test results for AA6082/B<sub>4</sub>C and AA6082/SiC composites.

Figure 12 represents that the un-reinforced aluminum alloys have more impact strength than the reinforced composite and with the increase in the wt% of reinforcements; the impact strength goes in declining stage. This reduction in the impact strength with the percentage reinforcement is very marginal. The impact strength of base alloy is 9.5



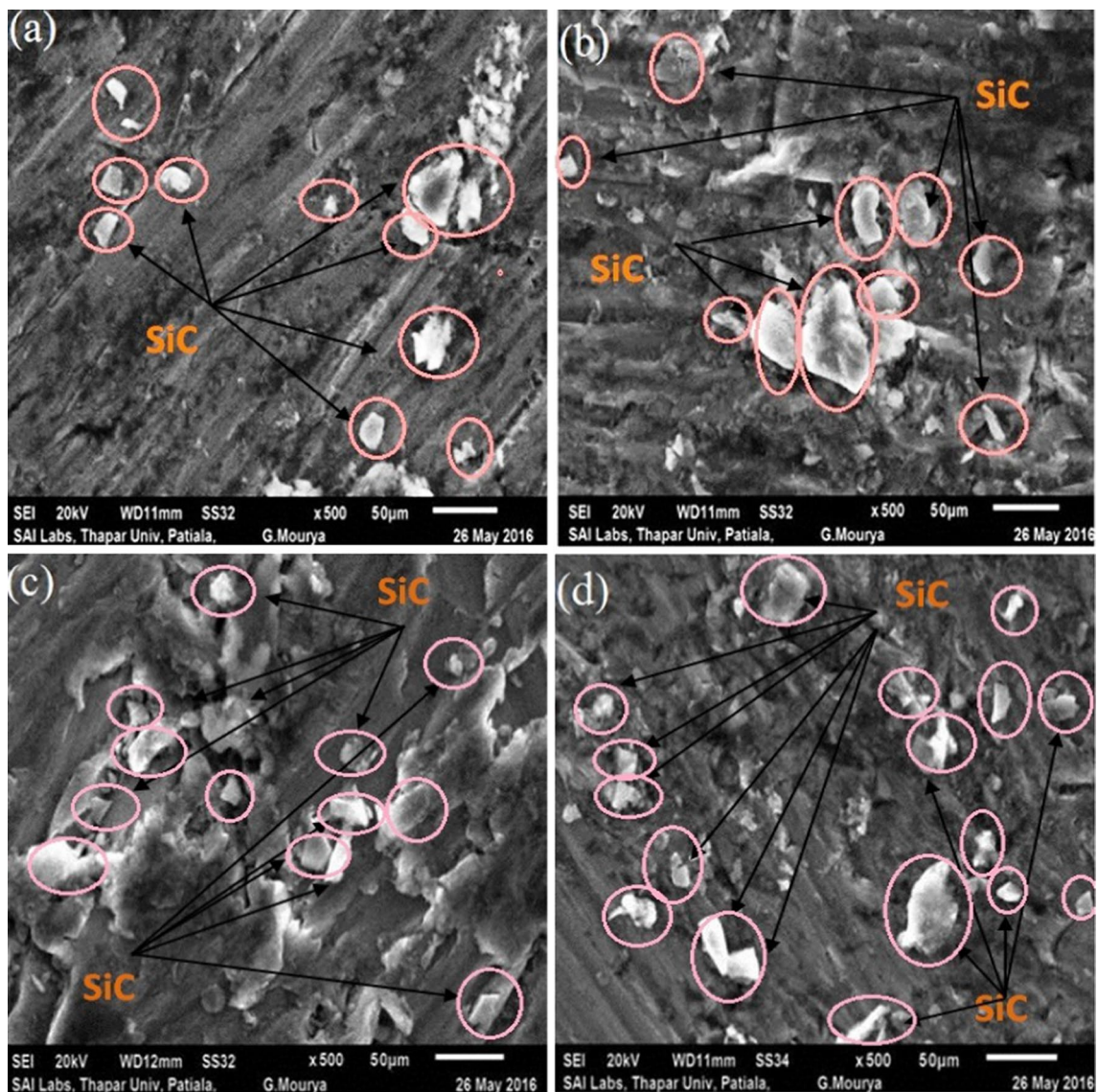


**Fig. 8** SEM micrographs for **a** 5%, **b** 10%, **c** 15% and **d** 20% of AA6082/SiC composites

**Table 4** Micro hardness of AA6082/B<sub>4</sub>C composites

Nomenclature of sample	HV 1	HV 2	HV 3	HV average	% Improvement (compared to base alloy)
Alloy + 5% B <sub>4</sub> C	104	103	105	104	3
Alloy + 10% B <sub>4</sub> C	112	113	112	112	10.9
Alloy + 15% B <sub>4</sub> C	118	117	116	117	15.8
Alloy + 20% B <sub>4</sub> C	115	115	115	115	13.86

Nm and the addition of B<sub>4</sub>C particulate (from 5 to 20%) decreases its strength up to 8.0 Nm. The impact strength of AA6082/SiC composite reduced up to 7.6 Nm. This reduction is attributed due to the addition of hard particles in the aluminum matrix. There is also slight transformation

in the nature of material from ductile to brittle with the gradual addition of particulates in the aluminium matrix. Due to this transition the impact strength found to be decreased. [27].

**Table 5** Micro hardness of AA6082/SiC composites

Nomenclature of sample	HV 1	HV 2	HV 3	HV average	% Improvement (compared to base alloy)
Alloy + 5% SiC	102	104	103	103	2
Alloy + 10% SiC	107	108	117	107	6
Alloy + 15% SiC	111	111	111	111	10
Alloy + 20% SiC	114	112	114	113	11.9

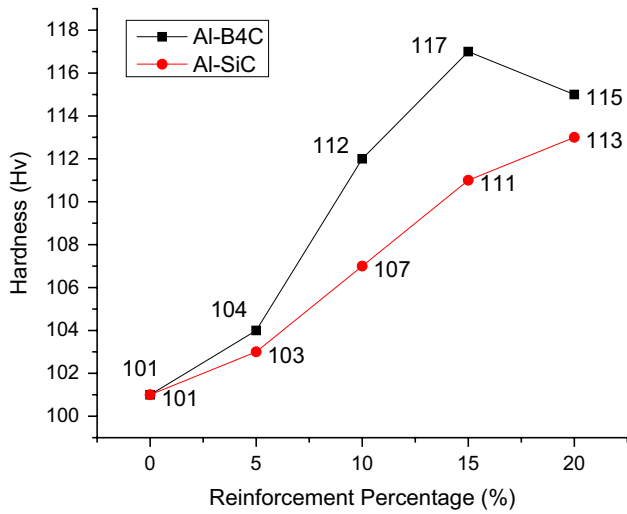


**Fig. 9** Hardness distributions for AA6082/B<sub>4</sub>C and AA6082/SiC composites

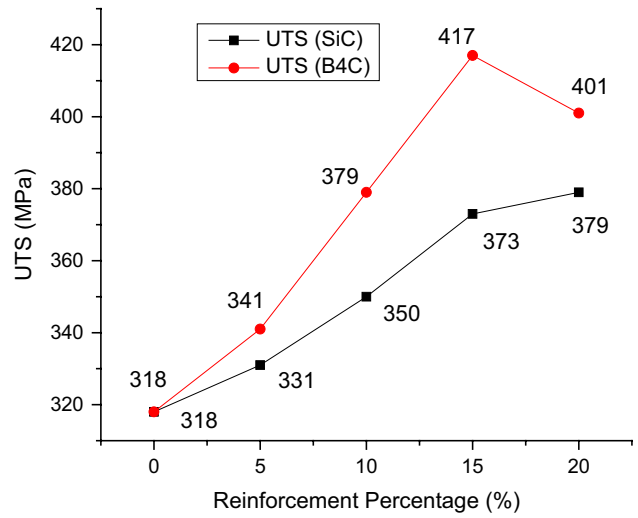


**Fig. 10** Variation of UTS for AA6082/SiC and AA6082/B<sub>4</sub>C composites

**Table 6** Tensile tests results with percentage elongation for AA6082/B<sub>4</sub>C composites

Nomenclature of sample	UTS (MPa)	% Improvement	% Elongation
Al alloy	318	–	8.38
Alloy + 5% B <sub>4</sub> C	341	7.2	8.01
Alloy + 10% B <sub>4</sub> C	379	19.1	7.7
Alloy + 15% B <sub>4</sub> C	417	31.1	7.4
Alloy + 20% B <sub>4</sub> C	401	26.1	7.3

**Table 7** Tensile tests results with percentage elongation for AA6082/SiC composites

Nomenclature of sample	UTS (MPa)	% Improvement	% Elongation
Al alloy	318	–	8.38
Alloy + 5% SiC	331	4.1	7.8
Alloy + 10% SiC	350	10	7.2
Alloy + 15% SiC	373	17.3	6.9
Alloy + 20% SiC	379	19.1	6.8

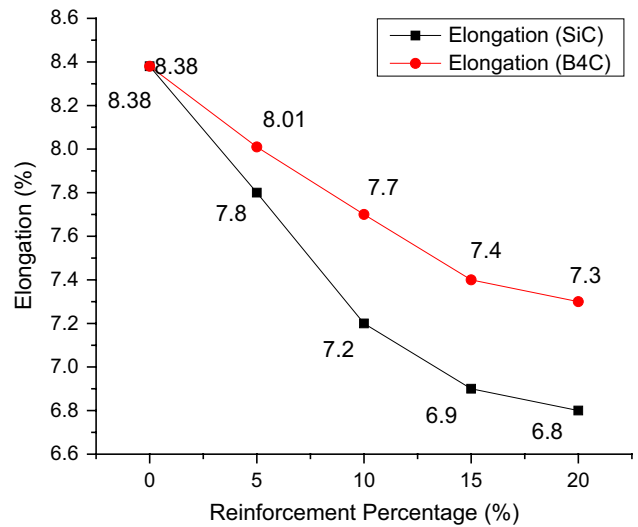


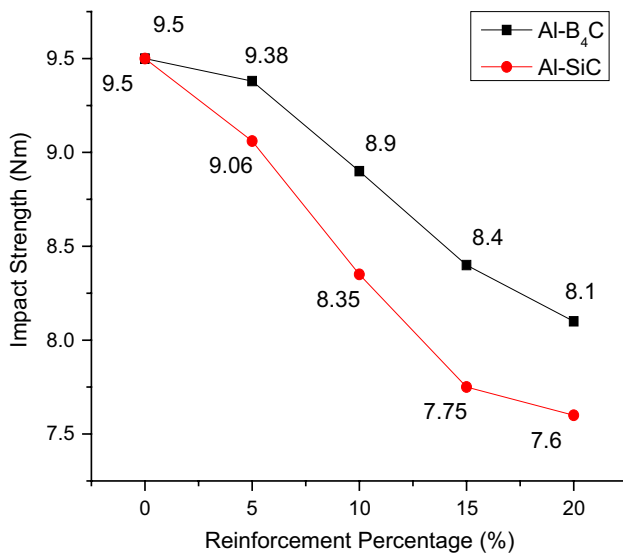
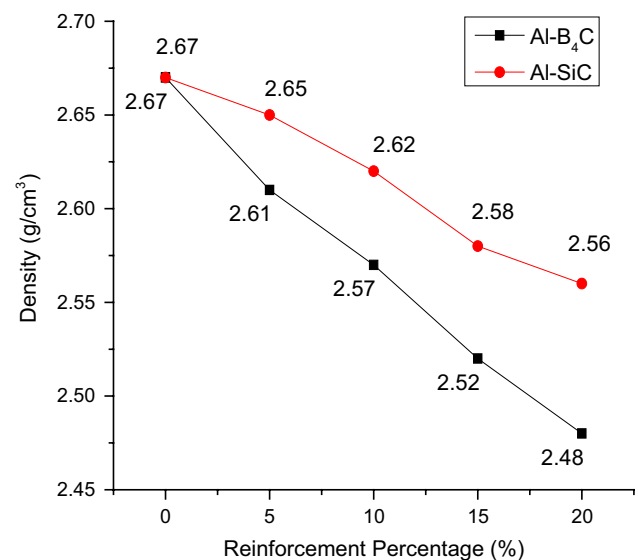
**Fig. 11** Variation of percentage elongation for AA6082/SiC and AA6082/B<sub>4</sub>C composites

**Table 8** Results of Impact Tests for AA6082/B<sub>4</sub>C composites

Nomenclature of sample	Trail 1 (Nm)	Trail 2 (Nm)	Trail 3 (Nm)	Average impact strength (Nm)
Al alloy	9.4	9.7	9.4	9.50
Alloy + 5% B <sub>4</sub> C	9.3	9.3	9.4	9.33
Alloy + 10% B <sub>4</sub> C	8.8	8.10	8.9	8.9
Alloy + 15% B <sub>4</sub> C	8.3	8.3	8.6	8.4
Alloy + 20% B <sub>4</sub> C	8.0	8.1	8.1	8.0

**Table 9** Results of impact tests for AA6082/SiC composites

Nomenclature of sample	Trail 1 (Nm)	Trail 2 (Nm)	Trail 3 (Nm)	Average impact strength (Nm)
Al alloy	9.4	9.7	9.4	9.50
Alloy + 5% SiC	9.0	9.1	9.1	9.06
Alloy + 10% SiC	8.4	8.3	8.3	8.35
Alloy + 15% SiC	7.8	7.6	7.9	7.75
Alloy + 20% SiC	7.7	7.6	7.7	7.6

**Fig. 12** Impact strength variations for AA6082/B<sub>4</sub>C and AA6082/SiC composites**Fig. 13** Density variations for AA6082/B<sub>4</sub>C and AA6082/SiC composites

### 3.5 Density

The density of specimen was investigated using Eq. 3 as discussed in the “Materials and Methods” section. Figure 13 gives the variation in the density of B<sub>4</sub>C and SiC reinforced composites with the variation of gradual addition of the reinforcement. The density of AA6082/SiC composite decreases from 2.67 to 2.56 g/cm<sup>3</sup> with the increase of particulates in the metal matrix. The density was lowest when 20 wt% of SiC was added to the molten alloy. It was found that the addition of B<sub>4</sub>C particulates at

20 wt% reduces the density of composites to the lowest value of 2.48 g/cm<sup>3</sup>. This decrement in the density value was 4.1% in AA6082/SiC and 7.1% in AA6082/B<sub>4</sub>C composites respectively as compared to the base alloy and this could be due to the density characteristics of particulates. Both particulates (SiC and B<sub>4</sub>C) exhibit low density values as compared to the aluminum base alloy. However, the addition of reinforcement has not change the density of the composites to a great extent. Similar observations for density in the aluminum composites were reported by the researchers in the past [28].

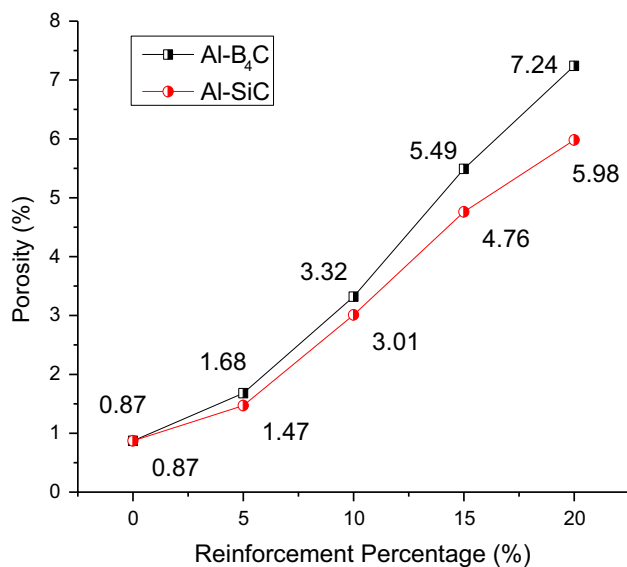


**Fig. 14** Porosity variations for AA6082/B<sub>4</sub>C and AA6082/SiC composites

### 3.6 Porosity

Figure 14 shows the variation in porosity for the AA6082/B<sub>4</sub>C and AA6082/SiC composites with increase in reinforcement. A slight affect was observed on the porosity of B<sub>4</sub>C and SiC reinforced composites after the blending of reinforcement particles. Porosity was observed to be higher in AA6082/B<sub>4</sub>C composites in which it raises to 7.24% in composite having 20 wt% of B<sub>4</sub>C as compared to 0.84% in base alloy. The porosity increase in AA6082/SiC composites is limited to 5.98% only. The chance of agglomeration in SiC composites is more due to their high density. So, in case of AA6082/SiC composites the probability of the formation of voids decreases as compared to AA6082/B<sub>4</sub>C composites. A similar observation for porosity in the aluminium composites was reported by the researchers in the past [28] As the results shows, the porosity in SiC reinforced is lower as compared to B<sub>4</sub>C reinforced composites. B<sub>4</sub>C particles exhibit low density value due to which boron-carbide particles can float in the upper and middle layer of mixture as compared to SiC particles. The chance of agglomeration increases in SiC due to their high density. Also the existence of the B<sub>4</sub>C particulate in the composite increases the little voids and cracks due to their low density.

## 4 Conclusions

The authors have drawn the following conclusions from the present work:

1. The successful production using the conventional stir casting process is attained for both the AA6082/B<sub>4</sub>C and AA6082/SiC composites with varying wt% of 0, 5, 10, 15 and 20.
2. X-ray diffraction patterns show the peaks of Al, Si and B<sub>4</sub>C along with Al<sub>3</sub>BC as by products in AA6082/B<sub>4</sub>C composites. In AA6082/SiC, the presence of Al, Si, SiC and Al<sub>4</sub>C<sub>3</sub> has been reported.
3. SEM micrographs reveal the homogeneity at different wt% of the reinforcement in the AA6082/B<sub>4</sub>C and AA6082/SiC composites beside with the existence of particle agglomeration at few places.
4. The addition of both B<sub>4</sub>C and SiC improves the micro hardness of the composites. The hardness rises due to the high solidity of particles in the low solidity of matrix containing aluminum alloy and reinforced particles. Since B<sub>4</sub>C is a high performance monolithic ceramic particle with enormously high solidity and low specific weight, it provides better resistance to deformation as compared to SiC. The maximum hardness is observed as 117 HV at the addition of 15 wt% of B<sub>4</sub>C and it goes down to 115 HV in composites having 20 wt% of B<sub>4</sub>C which could be due to the development of clusters within the composite at excessive addition of reinforced particles. The maximum hardness for AA6082/SiC is found to be 113 HV at adding 20 wt% of SiC in aluminum matrix. The expansion in the hardness for B<sub>4</sub>C and SiC reinforced composites is reported to be 15.8% and 11.9% respectively.
5. The UTS in the base alloy was 318 HV which increases to 417 HV at the addition of 15 wt% of B<sub>4</sub>C in AA6082/B<sub>4</sub>C composites which is an increase of 31% but further addition of B<sub>4</sub>C reduces the strength to 401 HV and the possible reason could be the particle agglomeration and increased porosity. The higher porosity results in the decrement of both the micro hardness and UTS of AA6082/B<sub>4</sub>C composite at higher reinforcement percentage. In case of AA6082/SiC composites, the UTS is reported as 379 HV at the addition of 20 wt% of SiC which give an increase of 19.1% in strength.
6. Reduction in Percentage elongation is observed in both the composites with the gradual addition of B<sub>4</sub>C and SiC and this is because of the resistance in the flow ability presented by the hard ceramic particles. The reduction is more in B<sub>4</sub>C reinforced composites.
7. The impact strength reduces from 9.5 Nm in base alloy to 8.1 Nm in AA6082/B<sub>4</sub>C and 7.6 Nm in AA6082/SiC composites respectively. This reduction is attributed due to the addition of hard particles in the aluminum matrix. There is also slight transformation in the nature of material from ductile to brittle with the gradual addition of particulates in the aluminium matrix.

8. Only slight variation in density is observed. Density reduces from 2.67 g/cm<sup>3</sup> in base alloy to 2.48 g/cm<sup>3</sup> in AA6082/B<sub>4</sub>C and 2.56 g/cm<sup>3</sup> in AA6082/SiC composites respectively which attributes to the density characteristics of particulates. The lower density of B<sub>4</sub>C particles as compared to SiC particles results in the lower density of AA6082/B<sub>4</sub>C composites as compared to AA6082/SiC composites.
9. Porosity is observed to be higher in AA6082/B<sub>4</sub>C composites in which it raises to 7.24% in composite having 20 wt% of B<sub>4</sub>C as compared to 0.84% in base alloy. The porosity increase in AA6082/SiC composites is limited to 5.98% only. The chance of agglomeration in SiC composites is more due to their high density. So, in case of AA6082/SiC composites the probability of the formation of voids decreases as compared to AA6082/B<sub>4</sub>C composites.

## References

1. W. Mocko, J.A. Rodriguez-Martinez, Z.L. Kowalewski, Compressive viscoplastic response of 6082-T6 and 7075-T6 aluminium alloys under wide range of strain rate at room temperature: experiments and modeling. *Strain* **48**, 498–509 (2012)
2. J.M. Lee, C.G. Lee, S.B. Kang, A. Kamio, A new technology for the production of aluminum matrix composites by the plasma synthesis method. *Met. Mater.* **6**(4), 389–394 (2000)
3. V. Vijayaraghavana, S. Castagne, Measurement of surface characteristics of Ti6Al4V aerospace engineering components in mass finishing process. *Measurement* **115**, 279–287 (2018)
4. G. Singh, S. Lap-Ip Chan, N. Sharma, Parametric study on the dry sliding wear behaviour of AA6082-T6/TiB<sub>2</sub> in situ composites using response surface methodology. *J. Braz. Soc. Mech. Sci. Eng.* **40**, 310 (2018)
5. R. Haghayeghi, E. Ezzatneshan, H. Bahai, RETRACTED ARTICLE: grain refinement of AA5754 aluminum alloy by ultrasonic cavitation: experimental study and numerical simulation. *Met. Mater. Int.* **21**(1), 109–117 (2015)
6. G. Singh, S. Goyal, Microstructure and mechanical behavior of AA6082-T6/SiC/B<sub>4</sub>C-based aluminum hybrid. *Compos. Part. Sci. Technol.* **36**, 154–161 (2018)
7. J.K. Chen, I.S. Huang, Thermal properties of aluminum-graphite composites by powder metallurgy. *Compos. Part B* **44**, 698–703 (2013)
8. A.R. Kennedy, The microstructure and mechanical properties of Al–Si–B<sub>4</sub>C metal matrix composites. *J. Mater. Sci.* **37**, 317–323 (2002)
9. K. Ravikumar, K. Kiran, V.S. Sreebalaji, Characterization of mechanical properties of aluminium/tungsten carbide composites. *Measurement* **102**, 142–149 (2017)
10. U.B. Gopal Krishna, K.V. Sreenivas Rao, B. Vasudeva, Effect of percentage reinforcement of B<sub>4</sub>C on the tensile property of aluminium matrix composites. *Int. J. Mech. Eng. Robot. Res.* **1**, 290–295 (2012)
11. D. Ghanbari, M.K. Asgarani, K. Amini, F. Gharavi, Influence of heat treatment on mechanical properties and microstructure of the Al2024/SiC composite produced by multi-pass friction stir processing. *Measurement* **104**, 151–158 (2017)
12. V.S. Aigbodion, S.B. Hassan, Effects of silicon carbide reinforcement on microstructure and properties of cast Al–Si–Fe/SiC particulate composites. *Mater. Sci. Eng. A* **447**, 355–360 (2007)
13. MdH Rahman, H.M. Mamun Al Rashed, Characterization of silicon carbide reinforced aluminum matrix composites. *Procedia Eng.* **90**, 103–109 (2014)
14. N.G. Siddesh Kumar, G.S. Shiva Shankar, S. Basavarajappa, R. Suresh, Some studies on mechanical and machining characteristics of Al2219/nB<sub>4</sub>C/MoS<sub>2</sub> nano-hybrid metal matrix composites. *Measurement* **107**, 1–11 (2017)
15. Z. Tan, Z. Chen, G. Fan, G. Ji, J. Zhang, R. Xu, A. Shan, Z. Li, D. Zhang, Effect of particle size on the thermal and mechanical properties of aluminum composites reinforced with SiC and diamond. *Mater. Des.* **90**, 845–851 (2016)
16. Y. Afkham, R.A. Khosroshahi, S. Rahimpour, C. Aavani, D. Brabazon, R.T. Mousavian, Enhanced mechanical properties of in situ aluminium matrix composites reinforced by alumina nanoparticles. *Arch. Civ. Mech. Eng.* **18**, 215–226 (2018)
17. M.C. Senel, M. Gurbuz, E. Koc, Fabrication and characterization of synergistic Al–SiC–GNPs hybrid composites. *Compos. B* **154**, 1–9 (2018)
18. G. Singh, S. Goyal, Dry sliding wear behaviour of AA6082-T6/SiC/B<sub>4</sub>C hybrid metal matrix composites using response surface methodology. *Proc. IMechE Part L J. Mater. Des. Appl.* **232**(11), 952–964 (2018)
19. H. Singh, M. Irfan Ul Haq, A. Raina, Dry sliding friction and wear behaviour of AA6082-TiB<sub>2</sub> in situ composites. *Silicon* (2019). <https://doi.org/10.1007/s12633-019-00237-y>
20. J. Hashim, L. Looney, M.S.J. Hashmi, The enhancement of wettability of SiC particles in cast aluminium matrix composites. *J. Mater. Process. Technol.* **119**, 329–335 (2001)
21. L. Poovazhagan, K. Kalaichelvan, A. Rajadurai, V. Senthilvelan, Characterization of hybrid silicon carbide and boron carbide nanoparticles-reinforced aluminum alloy composites. *Procedia Eng.* **64**, 681–689 (2013)
22. Y. Sahin, Preparation and some properties of SiC particle reinforced aluminium alloy composites. *Mater. Des.* **24**, 671–679 (2003)
23. J.K.M. Kwok, S.C. Lim, High speed tribological properties of some Al/SiC composites: I. Frictional and wear rate characteristics. *Compos. Sci. Technol.* **59**, 55–63 (1999)
24. T. Raviteja, N. Radhika, R. Raghu, Fabrication and mechanical properties of stir cast Al–Si<sub>12</sub>Cu/B<sub>4</sub>C composites. *Int. J. Res. Eng. Technol.* **3**, 343–346 (2014)
25. S. Gopalakannan, T. Senthilvelan, Synthesis and characterisation of Al 7075 reinforced with SiC and B<sub>4</sub>C nano particles fabricated by ultrasonic cavitations method. *J. Sci. Ind. Res.* **74**, 281–285 (2015)
26. A. Mazahery, M.O. Shabani, Mechanical properties of squeeze-cast A356 composites reinforced with B<sub>4</sub>C particulates. *J. Mater. Eng. Perform.* **21**(2), 247–252 (2012)
27. J.A. Jansen, Ductile-to-brittle transition of plastic materials. *Adv. Mater. Process.* **164**(2), 39–42 (2006)
28. K. Shirvanimoghaddam, H. Khayyam, H. Abdizadeh, M.K. Akbari, A.H. Pakseresht, E. Ghasali, M. Naebe, Boron carbide reinforced aluminium matrix composite: physical, mechanical characterization and mathematical modelling. *Mater. Sci. Eng. A* **658**, 135–149 (2016)

**Publisher's Note** Springer Nature remains neutral with regard to jurisdictional claims in published maps and institutional affiliations.